

# Viscoelastic Relaxation of Polyurethane at Different Stages of the Gel Formation. 1. Glass Transition Dynamics

Hery Randrianantoandro, Taco Nicolai,\* Dominique Durand, and Frederic Prochazka

*Chimie et Physique des Matériaux Polymères, UMR CNRS, Université du Maine, 72085 Le Mans Cedex 9, France*

*Received December 6, 1996; Revised Manuscript Received June 17, 1997*

**ABSTRACT:** We report results on the local segmental relaxation ( $\alpha$ -relaxation) of a cross-linked polyurethane system formed by polycondensation of a triol and a diisocyanate at different connectivity extents. Stable samples with different connectivity extents were obtained either by varying the amount of excess triol (A) or by addition of different amounts of a mono alcohol (B). The glass transition temperature ( $T_g$ ) increases linearly with increasing connectivity extent for system A, while for system B it is almost constant.  $T_g$  is thus mainly related to the amount of urethane groups. The temperature dependence of the  $\alpha$ -relaxation is independent of the connectivity extent and is the same for both systems. The shape of the  $\alpha$ -relaxation can be described by a stretched exponential which decreases with an increasing connectivity extent, but in a different way for both systems.

## Introduction

Much attention has been given in the recent past to the mechanical relaxation spectra of gel-forming systems around the gel point (e.g. refs 1–11). Most systems show a power law time dependence of the shear modulus close to the sol–gel transition. The viscosity before the gel point and the gel modulus after the gel point are found to scale with the parameter  $\epsilon$  which characterizes the approach to the gel point:  $\epsilon \equiv |p - p_c|/p_c$ , where  $p$  is the connectivity extent and  $p_c$  is the critical value at the gel point. The experimental results have generally been interpreted in terms of the classical mean field theory or the percolation model.

Most experimental studies were done over a limited dynamic range and only on systems close to the gel point. The limited dynamic range is imposed by the instrumental limits for systems that have to be studied in situ during the reaction. However, if stable systems can be produced at different stages of the gelation process, the experimental limitation can be overcome by measuring at different temperatures and applying a time–temperature superposition. For this reason we have studied the formation of polyurethane networks which result from a polycondensation reaction of poly(oxypropylene) triol with diisocyanate. By varying the stoichiometric ratio ( $r$ ) of the isocyanate and alcohol groups (method A) it is possible to obtain stable systems at all stages of the gel formation. An alternative method (B) is to add different fractions of monoalcohol keeping  $r = 1$  ( $f$  is the fraction of hydroxyl groups from triol). The second method means that we keep the total number of urethane groups constant throughout the gel formation. We investigated the system at different stoichiometries from the pure alcohol ( $r = 0$ ) to the fully grown gel ( $r = 1$ ) or alternatively from  $f = 0$  to  $f = 1$ . We have studied the frequency dependence of the shear modulus of these systems over a wide temperature range covering both the glass transition dynamics and the sol–gel transition dynamics.

In part 2,<sup>16</sup> we will present the results on the low-frequency (high-temperature) dynamics. Here we present the results of the glass transition dynamics. We have

already reported an investigation of the glass transition dynamics of a fully grown polyurethane gel in which we compared the results from ultrasonic spectroscopy (US), dynamic light scattering (DLS) and dynamical mechanical thermal analysis (DMTA).<sup>12</sup> Besides the main  $\alpha$ -relaxation, a secondary  $\beta$ -relaxation was observed by DMTA. The  $\alpha$ -relaxation was analyzed in terms of a so-called generalized exponential (GEX) relaxation time distribution, which can be made equivalent to a stretched exponential relaxation function ( $\exp(-(t/\tau_0)^\beta)$ ), and can be used both in the time and frequency domain.<sup>13</sup> The observed value of  $\beta$  was found to be 0.32 independent of the temperature in the small range investigated. The temperature dependence of the relaxation time is well described by the so-called Vogel–Fulcher equation with the same parameters for each technique if one takes into account that a modulus is measured by US and DMTA and a compliance by DLS.

We have also reported a study of the frequency dependence of pure poly(oxypropylene) triol and diol with different molar mass.<sup>14</sup> This study and earlier results from dielectric spectroscopy clearly show that the  $\alpha$ -relaxation and the internal modes relaxation do not have the same temperature dependence close to and below the glass transition temperature ( $T_g$ ). At these temperatures the  $\alpha$ -relaxation has a stronger temperature dependence. The  $\alpha$ -relaxation can again be characterized by a stretched exponential decay with  $\beta = 0.49$  independent of the temperature and the molar mass. The internal modes relaxation is well described by the Rouse model.

## Experimental Section

Polyurethanes were formed by condensation of poly(oxypropylene) (POP) triol with hexamethylene diisocyanate (HMDI). The polyols used in this study are propylene oxide adducts of trimethylolpropane. The number-average molar mass of the triol is 720 g/mol and the hydroxyl content is  $4.16 \times 10^{-3}$  mol/g, which leads to an effective functionality of the polyol close to three. After the dried triol was mixed with HMDI in the appropriated stoichiometric ratio,  $2 \times 10^{-3}$  g of dibutyl tin dilaurate catalyst was added for every gram of HMDI in the form of a 2% (w/w) solution in toluene. After mixing and complete homogenization of the reaction components, the sample was cured at 40 °C until complete consumption of the isocyanate groups occurred. Samples at different connectivity extents were prepared by following two methods: (A) samples

\* Abstract published in *Advance ACS Abstracts*, September 1, 1997.

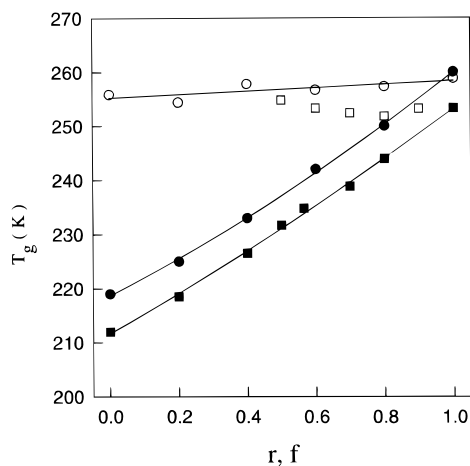


**Figure 1.** Glass transition temperature as a function of  $r$  for system A (filled symbols) and as a function of  $f$  for system B (open symbols). The circles represent values obtained from DSC ( $T_{gc}$ ) while the squares represent the temperatures where  $\omega_{\max} = 1$  rad/s ( $T_{gv}$ ).

were prepared at different stoichiometric ratios ( $r$ ) defined as the initial ratio of isocyanate groups [NCO] to hydroxyl groups [OH]; (B) samples were prepared at different ratios of polyoxypropylene triol and phenyl-2-propanol at  $r = 1$ .  $f$  is defined as the fraction of alcohol groups belonging to POP triol. The critical values at the gel point are  $r_c = 0.569$  and  $f_c = 0.596$ .

Calorimetric glass transition temperatures,  $T_{gc}$ , were measured using differential scanning calorimetry. The samples were cooled rapidly to 100 K and then heated at a rate of 10 deg/min. Values of  $T_{gc}$  taken as the midpoint of the transition are plotted as a function of  $r$  and  $f$  in Figure 1. The reproducibility is  $\pm 2$  °C. The presence of a small amount of toluene used to facilitate the addition of catalyst, decreases  $T_g$  by at most 5 °C compared to a system to which pure catalyst was added.

Dynamic shear measurements were done on a Rheometrics RDA II dynamic spectrometer using parallel-plate geometry at temperatures between 200 and 340 K. In the so-called hold mode the gap is corrected for temperature variations of the sample volume. The plate size (diameter between 50 and 4 mm) and the imposed deformation (0.2–20%) were adjusted to obtain an accurate torque response while remaining in the linear regime. The shear modulus could be measured in the range  $10^{-10}$  Pa. We were able to measure very large moduli by using the maximum stable sample thickness (2–2.5 mm) in combination with a small plate size.

## Results and Discussion

**Glass Transition Temperature.** Figure 1 shows the glass transition temperatures as a function of connectivity extent ( $r$  or  $f$ ) for the two systems. For each system two values are shown: one obtained from DSC ( $T_{gc}$ ) and one defined as the temperature where the maximum loss shear modulus is at 1 rad/s ( $T_{gv}$ ). There is a systematic difference of about 6 °C between the two values, but the dependence on the connectivity extent is the same.  $T_{gv}$  values for the system made following method B for  $f < 0.5$  are not shown because in this range the system crystallizes partly which influences the shear modulus. The extent of crystallization decreases with increasing triol content and is no longer observed for  $f = 0.5$ .

System B has only a very weak dependence of  $T_g$  on the connectivity extent compared to system A for which  $T_g$  increases almost linearly with  $r$ . These observations indicate that the variation of  $T_g$  is dominated by the linear increase of the concentration of urethane groups with connectivity extent for method A. The weak influence of variation in the number of end groups and

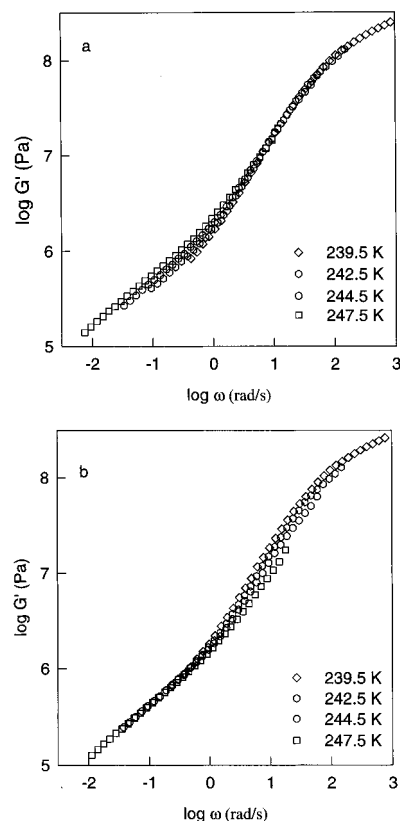


**Figure 2.** Time-temperature superposition of the storage shear modulus data at high (a) and low frequencies (b) of system A at  $r = 0.570$ .

cross-links is in agreement with measurements on pure poly(oxypropylene) triol and diol with different molar mass. These measurements show a weak variation of  $T_g$  with the molar mass even for very low molar masses, which is possibly due to hydrogen bonding.

**Shear Modulus.** The frequency dependence of the storage shear modulus ( $G'$ ) at  $r = 0.570$  is shown in Figure 2. In Figure 2a the data are superimposed at high frequencies while in Figure 2b they are superimposed at low frequencies. As was mentioned above, the  $\alpha$ -relaxation has a stronger temperature dependence than the internal modes relaxation close to and below  $T_g$ . We have discussed this feature in detail for the case of pure poly(oxypropylene)triol and -diol with different molar masses. The effect is the same at all connectivity extents. Of course, it renders a simple time-temperature superposition impossible. In this paper we concentrate on the  $\alpha$ -relaxation so that all data are superimposed at high frequencies. The data superimpose well over the small temperature range where the  $\alpha$ -relaxation is visible in the experimental window. This means that the shape of the  $\alpha$ -relaxation does not change significantly in this temperature range.

Figure 3 shows normalized master curves of the frequency dependence of the shear loss modulus ( $G''$ ) at different values of  $r$ . It is clear that the distribution broadens with increasing connectivity extent. The data have been analyzed by simultaneous fitting of both  $G'$  and  $G''$  to the GEX function

$$G'(\omega) = G_{\infty} \int_0^{\infty} A_g(\tau) \frac{\omega^2 \tau^2}{1 + \omega^2 \tau^2} d\tau \quad (1)$$

$$G''(\omega) = G_{\infty} \int_0^{\infty} A_g(\tau) \frac{\omega \tau}{1 + \omega^2 \tau^2} d\tau$$

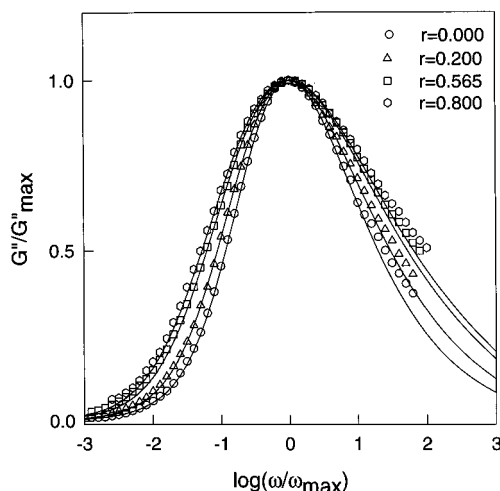


**Figure 3.** Normalized master curves of the loss shear modulus as a function of the frequency at different values of  $r$  indicated in the figure. The solid lines represent nonlinear least-squares fits to eqs 1 and 2 for  $\omega < 10\omega_{\max}$ .

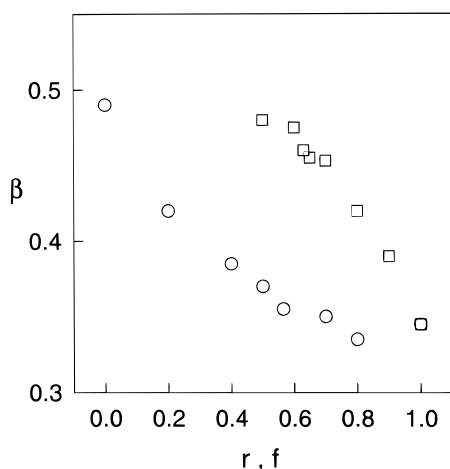


**Figure 4.** Values of the stretched exponent  $\beta$  which characterizes the shape of the  $\alpha$ -relaxation as a function of  $r$  and  $f$ .

with

$$A_g(\tau) = k\tau^{p-1} \exp[-(\tau/\tau_g)^s] \quad (2)$$

where  $G_\infty$  is the high frequency modulus, and  $k$  is a normalization constant such that  $\int A_g(\tau) d\tau = 1$ . A detailed discussion of this function and the comparison with the Havriliak–Negami and stretched exponential functions is given elsewhere.<sup>13</sup> The latter two empirical functions are much used in the literature to describe the  $\alpha$ -relaxation in the frequency and time domain, respectively. The GEX function is equivalent to a stretched exponential for  $\beta < 0.6$  if  $p = \beta$  and  $s = \beta/(1 - \beta)$ .

The solid lines in Figure 3 represent the results of nonlinear least-squares fits using eqs 1 and 2 and fixing  $s = p/(1 - p)$  so that the GEX function is equivalent to a stretched exponential. The stretched exponential gives a good description of the data for  $\omega < 10\omega_{\max}$ . At higher frequencies the data deviate indicating perhaps the influence of a secondary relaxation process. In the fits only data at  $\omega < 10\omega_{\max}$  were taken into account. The values of  $\beta$  are plotted as a function of the connectivity extent in Figure 4.  $\beta$  decreases rapidly from  $r = 0$  to  $r = 0.5$  and then stabilizes at a values of about 0.33. This last value is in agreement with the DLS and DMTA measurements reported in ref 12.  $G_\infty$

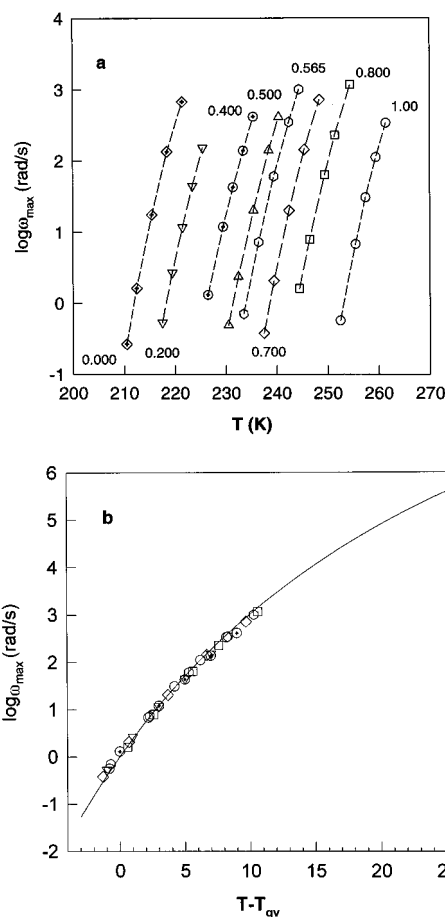


**Figure 5.** (a) Temperature dependence of  $\omega_{\max}$  for different values of  $r$  indicated in the figure. (b) Same data as in part a plotted as a function of  $T - T_{gv}$ . The solid line represents a fit to the Vogel–Fulcher equation of the combined results obtained for  $r = 1$  by DLS, US, and DMTA.

$= (5 \pm 1) \times 10^8$  Pa independent of the connectivity extent. DMTA measurements of the Young modulus for  $r = 1$  gave  $E_\infty = 1.4 \times 10^9$  Pa which is, as expected, about three times  $G_\infty$ .

The data for the system obtained by method B were analysed in the same way and the values of  $\beta$  are also shown in Figure 4. As mentioned above, for values of  $f < 0.5$  the system crystallizes so that only values at larger  $f$  are shown. The value of  $\beta$  is systematically larger for system B except very close to the fully grown gel. The systems obtained by method A at  $r = 1$  and by method B at  $f = 1$  are, of course, the same.

In Figure 5a we have plotted the temperature dependence of  $\omega_{\max}$  at different values of  $r$ . And in Figure 5b, the same data are plotted as a function of  $T - T_{gv}$ . It is clear that the temperature dependence is independent of the connectivity extent over the limited range experimentally accessible. The temperature dependence is the same as that observed by other techniques over a much wider temperature range at  $r = 1$ <sup>12</sup> and can be described by the so-called Vogel–Fulcher equation:  $\omega_{\max} = \omega_\infty \exp(-B/(T - T_0))$ . The temperature dependence of  $\omega_{\max}$  for system B at different values of  $f \geq 0.5$  is the same as for system A if plotted as a function of  $T - T_{gv}$ .

Böhmer et al. noted an empirical correlation between the width of the  $\alpha$ -relaxation and the fragility of the glass defined as  $m = 16 + 590T_0/B$ .<sup>15</sup> For both systems  $B \approx 1050$  is independent of the connectivity extent. For system A,  $T_0 \approx T_{gc} - 42$  increases as a function of the

connectivity extent so that the fragility increases while  $\beta$  decreases in qualitative accordance with the observed correlation. However, for  $r > 0.5$  the value of  $\beta$  is almost constant while  $m$  continues to increase. For system B the fragility is independent of the connectivity extent, at least for  $f \geq 0.5$ , but  $\beta$  decreases sharply from about 0.45 to 0.35 when  $f$  approaches unity. It is clear that for these systems there is no simple correlation between the width of the  $\alpha$ -relaxation and the fragility of the glass.

**Acknowledgment.** We thank J. F. Tassin for his support with the dynamic shear measurements.

## References and Notes

- (1) Eloundou, J. P.; Fève, M.; Gerard, J. F.; Harran, D.; Pascault, J. P. *Macromolecules* **1996**, *29*, 6907.
- (2) Yu, J. M.; Dubois, Ph.; Teyssié, Ph.; Jérôme, R.; Blacher, S.; Brouers, F.; L'Homme, G. *Macromolecules* **1996**, *29*, 5384.
- (3) Winter, H. H.; Chambon, F. *J. Rheol.* **1986**, *30*, 367.
- (4) Chambon, F.; Petrovic, Z. S.; MacKnight, W. J.; Winter, H. H. *Macromolecules* **1986**, *19*, 2146.
- (5) Axelos, M. A. V.; Kolb, M. *Phys. Rev. Lett.* **1990**, *64*, 1457.
- (6) Adolf, D.; Martin, J. E. *Macromolecules* **1991**, *24*, 6721.
- (7) Michon, C.; Cuvelier, G.; Launay, B. *Rheol. Acta* **1993**, *32*, 94.
- (8) Hodgson, D. F.; Amis, E. J. *Macromolecules* **1990**, *23*, 2512.
- (9) Matejka, L. *Polym. Bull.* **1991**, *26*, 109.
- (10) Matsumoto, T.; Masahiro, M.; Masuda, T. *Macromolecules* **1992**, *25*, 5430.
- (11) Prochazka, F.; Nicolai, T.; Durand, D. *Macromolecules* **1996**, *29*, 2260.
- (12) Tabellout, M.; Baillif, P. Y.; Randrianantoandro, H.; Litzinger, F.; Emery, J. R.; Nicolai, T.; Durand, D. *Phys. Rev. B* **1995**, *51*, 12295.
- (13) Nicolai, T.; Gimel, J. C.; Johnsen, R. *J. Phys II (Fr.)* **1996**, *6*, 697.
- (14) Randrianantoandro, H.; Nicolai, T. *Macromolecules*, in press.
- (15) Böhmer, R.; Angell, C. A. In *Disorder Effects on Relaxational Processes*; Richert, R., Blumen, A., Eds.; Springer-Verlag: Berlin, 1995.
- (16) Nicolai, T.; Randrianantoandro, H.; Prochazka, F.; Durand, D. *Macromolecules* **1997**, *30*, 5897.

MA961792D